UDC 621.315.592.3 DOI: 10.15222/TKEA2023.3-4.52

O. I. KONDRIK, D. A. SOLOPIKHIN

Ukraine, Kharkiv, National Science Center "Kharkiv Institute of Physics and Technology"
E-mail: kondrik@kipt.kharkov.ua

INFLUENCE OF THE CONTENT OF IMPURITIES AND STRUCTURAL DEFECTS ON THE PROPERTIES OF THE $Cd_{0.9}Mn_{0.1}Te$:V-BASED DETECTOR

The paper highlights the results of quantitative studies of the influence of the content of impurities and structural defects on the electrophysical and detector properties of $Cd_{0.9}Mn_{0.1}Te$:V — resistivity and concentrations of free charge carriers, life time of nonequilibrium charge carriers τ, charge collection efficiency η. The optimal ranges of energy change and deep donor concentration, which ensure a high-resistive state and acceptable values of τ and η, are established. The authors study the compensation of cadmium vacancies with vanadium admixture.

Keywords: CdMnTe, detector properties, simulation, structure defects, deep levels.

Cadmium manganese telluride is a direct band gap II–VI compound semiconductor with wide forbidden band, adjustable lattice parameters and a Mn segregation coefficient close to 1. Thus, $Cd_{1-x}Mn_xTe$ (**CMT**) is one of the new CdTe-based materials currently being developed, and it is considered as a promising semiconductor material for X-ray and gamma-ray detectors designed to operate at room temperature [1–4]. The main problem in the development of radiation detectors based on CMT is to produce single crystals free of defects. Crystal defects and impurities introduce electrically active energy levels into the bandgap, which deteriorate the charge transport properties of the detector with a decrease in the lifetime of nonequilibrium electrons τ_n and holes τ_p due to trapping phenomena [5, 6] and, as a result, incomplete charge collection. CMT single crystals usually have structural defects such as Te inclusions [7], which significantly deteriorate the detector performance. Such defects, however, are effectively eliminated using multi-step post-growth annealing method [2] or by applying special thermal regime for three-zone tubular furnace [8]. The transport properties of CMT are also strongly influenced by point defects which, like tellurium inclusions, introduce the deep energy levels into the band gap of the semiconductor. Thus, the levels located inside the band gap (0.81–0.85 eV) were found in CMT crystals [9], and these traps together with deep donors (E_{DD}=0.78–0.84 eV), according to an earlier study [9], should play a significant role in the compensation in these materials, which was confirmed by model results [10]. It was also concluded that the high content of residual impurities in manganese is an obstacle to obtaining highly efficient CMT-based detectors [11]. Thus, CMT has limitations that prevent it from being fully utilized in the cost-effective production of large-volume homogeneous sensors.

The most detrimental structural defects for CMT transport characteristics are cadmium vacancies V_{Cd}^{2-}, which significantly reduce resistivity ρ, the lifetime of nonequilibrium charge carriers τ, and the charge collection efficiency η [10]. To compensate for these doubly charged defects, alloying impurities V, In, Al are introduced [9, 12–14]. Donor impurities of transition metals can also enter into the CMT matrix, which can significantly affect ρ, τ_n, τ_p, η. The radiation resistance of CdMnTe-based detectors may also depend on the initial state of the matrix: the degree of purity and structural perfection.

CdMnTe of detector quality possess a high resistivity ρ (≈10^{10} Ω·cm). It greatly complicates the experimental study of the influence of such micro-parameters for impurities and defects as the positions of their energy levels E_i in the band gap, the capture cross-sections of nonequilibrium charge carriers σ_i, and the concentrations N_i on the resistivity of the detector and its charge collection efficiency η. These micro-properties also significantly affect such important characteristics as the products of mobility μ_n by the lifetime τ_n for electrons $\mu_n \cdot \tau_n$ and those for holes $\mu_p \cdot \tau_p$. Simulation of "macroscopic" characteristics of detector materials (ρ, $\mu_n \cdot \tau_n$, $\mu_p \cdot \tau_p$, η) using "microscopic" parameters allows, by comparing the calculated values with experimentally measured "macrovalues", to understand the mechanisms of changes in the electrophysical and detector properties of CdMnTe depending on the concentration of impurities and defects. In this regard, the use of mathematical and computer modeling based on known experimental results and proven physical models as an additional research tool is quite relevant. The initial composition and "microscopic" parameters of CMT defects were experimentally studied in the most detail in paper [14] using the $Cd_{0.9}Mn_{0.1}Te$:V material. The results of this

ISSN 2225-5818 (Print)
ISSN 2309-9992 (Online)

work were taken as the basis and initial parameters for our model study.

The aim of the work was to determine by computer simulation the nature of the effect of background and alloying impurities and structural defects on the electrophysical and detector properties of $Cd_{0.9}Mn_{0.1}Te$.

Models and materials

The main parameters of the i^{th} deep levels of defects, which determine lifetime of nonequilibrium electrons and holes as well as charge collection efficiency in the $Cd_{0.9}Mn_{0.1}Te$-based detectors, experimentally studied in [14], are the Ni concentration, the capture cross-section σ_i and the position in the band gap (activation energy) E_i. Experimental studies of the band-to-band recombination rate in wide-gap semiconductors [15] showed that the capture and recombination of nonequilibrium electrons and holes at deep levels of impurities and defects have a decisive effect on their lifetime in such materials and, consequently, on the charge collection efficiency in detectors based on them. Therefore, to estimate the lifetime of nonequilibrium charge carriers, the Shockley–Read recombination model [16] was used. In [14], the TSC (thermally stimulated current) method was used to determine the capture cross sections σ_i, when the contribution of all levels to the currents emitted into the corresponding zones was simultaneously taken into account. These data made it possible to properly use the Shockley–Read model to calculate τ_n, τ_p correctly.

The applied models and their testing are described in detail in [17]. The electroneutrality equation was derived taking into account all impurities and defects experimentally registered in [14]. This equation has been solved numerically with respect to the Fermi level F, and concentrations of free electrons (n) and holes (p) were determined under parabolic zone approximation. The electron mobility μ_n was calculated under the pulse relaxation time approximation (tau approximation) with taking into account the scattering mechanisms at ionized and neutral centers, acoustic, piezoelectric and optic phonons. The mobility of holes μ_p was considered constant and equal to 100 $cm^2/(V \cdot s)$. The specific conductivity was calculated using the formula $e \cdot n \cdot \mu_n + e \cdot p \cdot \mu_p$, and the resistivity done as its reciprocal quantity. The charge collection efficiency of the detector was determined according to Hecht's equation [18, p. 489]. The distance between the detector electrodes was assumed to be 5 mm, and the electric field strength was 1000 V/cm.

The initial composition of technological and background impurities and defects in CMT was adopted mainly based on the results of paper [14], where the TSC method was used to study the $Cd_{0.9}Mn_{0.1}Te$:V (**CMT:V**) crystal grown by the Te solution vertical Bridgman method. The resulting composition, which is presented in the **Table** for sample CMT:V, ensured the achievement of a high-resistive state $\rho \approx 10^{10}$ Ω·cm at the concentration of the substitutional vanadium donor impurity of $1 \cdot 10^{16}$ cm^{-3}.

The first column of the table shows the levels of the CMT:V material, which are denoted in [14] by T_i. The second column shows the values of the concentrations of the corresponding defects, used in the model study. The third column shows the values of energy levels E_T and the fourth one — the capture cross sections σ of nonequilibrium charge carriers. Explanations of the nature of defects taken from [14] are displayed in the fifth column. The E_T energies of the donor defects levels (electron traps) are measured from the conduction band bottom,

Parameters of the deep trap levels obtained from the TSC spectrum by the SIMPA method in the $Cd_{0.9}Mn_{0.1}Te$:V crystal

Trap	Concentration, cm^{-3}	E_T, eV	σ, cm^2	Origins [14]
T_1	$\approx 1.0 \cdot 10^{15}$	0.077	$1.6 \cdot 10^{-22}$	Vanadium instead of cadmium V_{Cd}^{+}
T_2	$2.3 \cdot 10^{14}$	0.159	$1.2 \cdot 10^{-20}$	Dislocation related
T_3	$1.0 \cdot 10^{15}$	0.174	$1.5 \cdot 10^{-20}$	$[O_{Te}^{-} V_{Cd}]^{-/2-}$ complex
T_4	$7.9 \cdot 10^{15}$	0.254	$7.2 \cdot 10^{-18}$	Acceptor structural defects
T_5	$2.6 \cdot 10^{15}$	0.278	$1.6 \cdot 10^{-17}$	Donor V-related electron trap
T_6	$6.9 \cdot 10^{14}$	0.294	$1.1 \cdot 10^{-17}$	Acceptor X level
T_7	$2.9 \cdot 10^{14}$	0.320	$6.0 \cdot 10^{-18}$	Te_{Cd} complex
T_8	$1.8 \cdot 10^{14}$	0.350	$6.9 \cdot 10^{-18}$	$[Te_{Cd}^{-2} V_{Cd}]$ complex
T_9	$7.0 \cdot 10^{14}$	0.447	$9.9 \cdot 10^{-17}$	V_{Cd}^{+}-related defects
T_{10}	$2.6 \cdot 10^{14}$	0.460	$1{,}7 \cdot 10^{-17}$	$[Te_{Cd}^{-2} V_{Cd}]^{2-/-}$ complex
T_{11}	$4.1 \cdot 10^{14}$	0.512	$9.9 \cdot 10^{-18}$	Cadmium vacancies V_{Cd}^{2-}
T_{12}	$4.8 \cdot 10^{15}$	0.620	$6.3 \cdot 10^{-18}$	Mn-related
T_{13}	$1.3 \cdot 10^{16}$	0.650	$3.0 \cdot 10^{-17}$	V-related hole trap
E_{DD}	$1.3 \cdot 10^{16}$	0.960	$1.0 \cdot 10^{-18}$	Deep donor energy derived from dark current characteristics

and those of acceptors (hole traps) are measured from the valence band top. The width of the band gap E_G for $Cd_{1-x}Mn_xTe$ at a room temperature of 20°C was determined by the formula $E_G = 1.45 + 1.45x$ eV [19]. After entering the composition of impurities and defects indicated in the Table into the model program, the electrophysical properties of $Cd_{0.9}Mn_{0.1}Te$:V were calculated for the vanadium concentration $N(V) = 1.25 \cdot 10^{16}$ cm^{-3} at $T = 20$°C, which turned out to be close to the values measured experimentally in [14]. The calculations allowed obtaining the electronic conductivity with the ratio $n/p = 20$, resistivity $\rho = 6.65 \cdot 10^{10}$ Ω·cm, the product of electron mobility by the lifetime of nonequilibrium electrons $\mu_n \cdot \tau_n = 4.8 \cdot 10^{-4}$ cm^2/V.

Results and discussions

Despite the results published in some papers [2, 9, 13, 14], accurate experimental measurement of impurity and defect concentrations in wide-band CdMnTe is still unattainable due to the high resistivity ($\approx 10^{10}$ Ω·cm) of the detector quality material. Therefore, to quantitatively study the electrophysical and detector properties of $Cd_{0.9}Mn_{0.1}Te$:V, the resistivity of this material was modeled depending on the change in its composition. The highly resistive state of $Cd_{0.9}Mn_{0.1}Te$ necessary for the detector was achieved by compensating its intrinsic acceptor defects (in particular, doubly charged cadmium vacancies V_{Cd}^{2-}) by introducing a shallow donor impurity [9]. Vanadium acted as such an admixture. But the main contribution to obtaining a semi-insulating material is made by a deep donor marked in the table by T_{14}. Its energy level of 0.96 eV relative to the conduction band was measured experimentally in [14]. It is of interest to investigate the behavior of ρ in $Cd_{0.9}Mn_{0.1}Te$:V within wide ranges of energies and concentrations of the deep donor. **Fig. 1** shows the three-dimensional dependence of the decimal logarithm of the resistivity of the referred above detector material on the concentration of deep donor and its energy level position in the band gap. The figure demonstrates that the maximum possible resistivity of the studied material can reach $3 \cdot 10^{11}$ Ω·cm, although in [14] the largest measured value ρ of the middle part of the ingot was $6.185 \cdot 10^{10}$ Ω·cm (see section 3.3.1). The maximum $\rho = 2.938 \cdot 10^{11}$ Ω·cm was reached at the donor energy $E_{DD} = 0.843$ eV relative to the top valence band, or $E_{DD} = 0.752$ eV, counted from the conduction band. And the minimal $\rho \geq 10^{10}$ Ω·cm necessary for detector-quality material was achieved at $E_{DD} = E_V + 0.743$ eV.

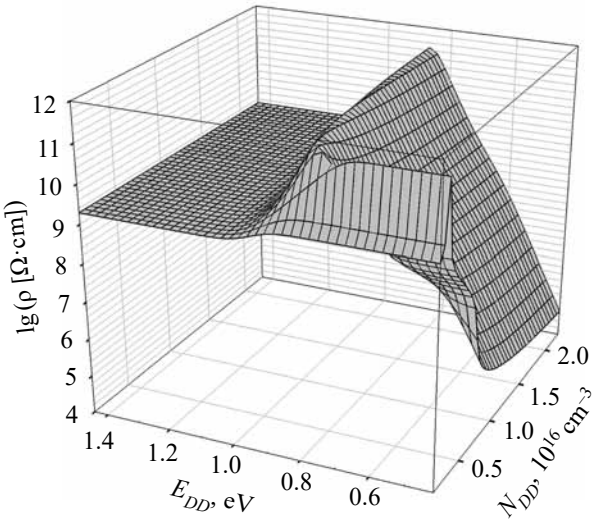

Fig. 1. Dependence of the resistivity of $Cd_{0.9}Mn_{0.1}Te$:V on the energy and concentration of the deep donor at the temperature of 20°C (the energy E_{DD} is counted relative to the top of valence band E_V)

Fig. 1 also shows that there are two extended maximums of ρ, the main being at $E_{DD} = 0.86$ eV and the secondary one at $N_{DD} = 2.5 \cdot 10^{15}$ cm^{-3}, which are almost identical in height. The first appears due to the compensation of acceptor levels by deep donors represented by the T_{14} level as well as T_{12}. The main contribution to the achievement of the high-resistance state is provided by T_{14}, but a certain influence is also exerted by the deep donor level of T_{12}. The latter, according to the authors [14], is related to the introduction of manganese. The second extended maximum occurs due to the compensation of shallow acceptor levels T_2, T_3, T_4 by the total number of donors, primarily by the vanadium impurity. The change of V content only by $1 \cdot 10^{14}$ cm^{-3}, causes a decrease in the value of ρ in this maximum by approximately one order of magnitude. In this way, it is almost impossible to get into the zone of high ρ of lateral maximum by changing the content of N_{DD} or alloying vanadium due to the too narrow range of the corresponding concentrations. It can also be seen that the existence of the lateral maximum does not depend on the E_{DD} energy of the level T_{14} at the energy $E_{DD} \geq 0.86$ eV, when its position in the band gap becomes not deep enough to ensure the highly resistive state of the detector material. Under these conditions, there is also a compensation of deep acceptors, primarily T_{13}, by deep donors with energy levels from 0.85 to 1.4 eV relative to the valence band. In this case, there is a fairly wide plateau with a resistivity of $2 \cdot 10^9$ Ω·cm and an electronic conductivity that may be required for the corresponding devices.

It should be noted that one of the problems of producing detector-quality high-resistance CdMnTe materials is the compensation of the effect of acceptor defects, especially cadmium vacancies V_{Cd}^{2-} with electronic conductivity at $n \geq p$. **Fig. 2** shows the three-dimensional dependences in the concentration of electrons n and holes p on the energy E_{DD} and concentration of the deep donor N_{DD}. (The range of N_{DD} change is the same as in Fig. 1, and the E_{DD} varies within 0.2 – 1.2 eV.)

Fig. 2, *a* shows a gentle plateau in the dependence of $\lg n\,(E_{DD}, N_{DD})$ when N_{DD} changes within $(2-5) \cdot 10^{15}$ cm^{-3} and E_{DD} within 1,0 – 1.2 eV. This plateau arises due to the process of the total compensating

ISSN 2225-5818 (Print)
ISSN 2309-9992 (Online)

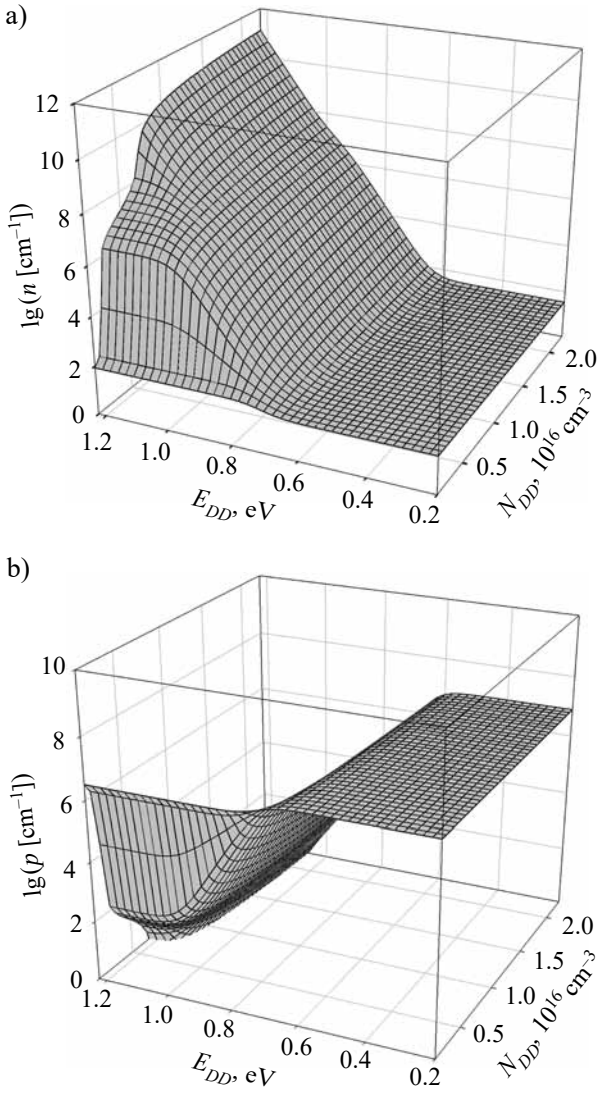

Fig. 2. Dependences of the concentrations of electrons (*a*) and holes (*b*) of $Cd_{0.9}Mn_{0.1}Te$:V on the energy and concentration of the deep donor at the temperature of 20°C (the energy E_{DD} is counted relative to the top of valence band E_V)

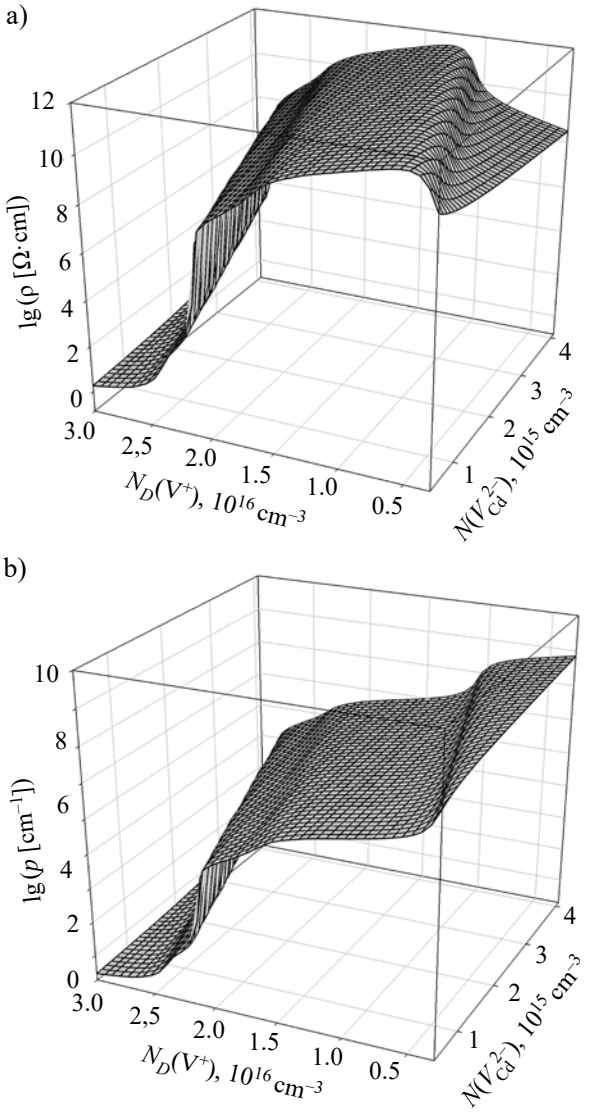

Fig. 3. Dependences of the resistivity (*a*) and concentration of free holes (*b*) of $Cd_{0.9}Mn_{0.1}Te$:V on the concentrations of acceptor defects of cadmium vacancies and shallow donor vanadium impurities

effect of V_{Cd}^{2-} cadmium vacancies by vanadium impurities and donor defects with the energy $E_{DD} > E_V + 1.0$ eV. In Fig. 2, *b* in the dependence of $\lg p(E_{DD}, N_{DD})$ in the specified ranges of E_{DD} and N_{DD} changes, a corresponding gentle plateau is also observed, but with an inverted slope. The flat surfaces in these pictures at $E_{DD} < E_V + 0.65$ eV characterize the low-resistance state of the material with hole conductivity.

To reduce the background noise of the detector, a material with hole conductivity and high-resistive state of $\approx 10^{10}$ Ω·cm is needed. The analysis of the model research showed that this condition for $Cd_{0.9}Mn_{0.1}Te$:V is satisfied at the deep donor concentration of $1 \cdot 10^{16}$ Ω·cm and within the range of its energies relative to the valence band $0.70 < E_{DD} < 0.775$ eV. Under these conditions, the p/n ratio is within 20–200, and ρ varies within $(0.5–5.0) \cdot 10^{10}$ Ω·cm. According to the vast majority of researchers, it is the doubly charged cadmium vacancies V_{Cd}^{2-}, which can reduce the specific resistance and charge collection of the detector, have the most negative effect on the operational characteristics of such material. **Fig. 3** shows the dependence of the specific resistance of $Cd_{0.9}Mn_{0.1}Te$:V and the concentration of free holes on the concentration of doubly charged cadmium vacancies V_{Cd}^{2-} and the donor impurity of vanadium. The concentration of the deep donor T_{14} (see the Table) is $1.3 \cdot 10^{16}$ cm^{-3}. The maximal theoretically possible resistivity reaches $3 \cdot 10^{11}$ Ω·cm. Fig. 3 also shows that the value of ρ is significantly affected by the content of the vanadium impurity which acts as a compensating shallow donor for cadmium vacancies T_{11} and hole trap T_{13}. When the vanadium content increases by only one order of magnitude, that is from $3 \cdot 10^{15}$ to $3 \cdot 10^{16}$ cm^{-3}, the value of ρ decreases by at least 10 orders of magnitude. At the same

time, the concentration of free holes increases rapidly (see Fig. 3, *b*) due to the influence of uncompensated acceptors, both shallow and deep ones. The high-resistance state is demonstrated by wide plateaus in Fig. 3 *a*, *b*. Compensation of V_{Cd}^{2-} is displayed in both figures by an inclined plane to the left of the high-resistance state. The compensation of the T_{13} hole trap is demonstrated by a gentle plateau with $\rho = 10^8 - 10^9$ Ω·cm to the right of the region of maximal ρ. In this high-resistance region, which is not always suitable for a detector-quality material, pure hole conduction occurs with the ratio $p/n \approx 0{,}8 \cdot 10^7$.

To complete the study, the influence of cadmium vacancies on the collection of detector charges should be investigated within the framework of the adopted model. **Fig. 4** shows the dependence of charge collection efficiency η on the concentration of the vanadium impurity for different contents of cadmium vacancies. In the calculations, the starting point of the drift of nonequilibrium charges was located in the immediate vicinity of the cathode at the distance of 0.5 mm. For this reason, the main contribution to the signal and the value of η was given by the drift of nonequilibrium electrons, and the maximal value of the charge collection efficiency was about of 0.7 (see Fig. 4). In the case when the starting point of charge drift was at the middle of the inter-electrode distance of the flat detector, the value of η did not exceed 0.55, which is significantly less than in $Cd_{0.9}Zn_{0.1}Te$, where η quantity in the initial state was about 0.9 [20]. The initial concentration of V_{Cd}^{2-} (curve *1*) was taken equal to $4.1 \cdot 10^{14}$ cm^{-3}, as measured in [14], with its gradual increase to $5 \cdot 10^{16}$ cm^{-3}. In the range of the vanadium content changes mentioned in Fig. 4, the largest resistivity of $Cd_{0.9}Mn_{0.1}Te$:V in the initial state ($N(V_{Cd}^{2-}) = 4.1 \cdot 10^{14}$ cm^{-3}) is observed at $N_D(V^+) = (5-6) \cdot 10^{15}$ cm^{-3} and is equal to $3 \cdot 10^{11}$ Ω·cm. However, even at $N(V_{Cd}^{2-}) = 1 \cdot 10^{16}$ cm^{-3} $\rho = 5 \cdot 10^7$ Ω·cm, and at $N(V_{Cd}^{2-}) = 2 \cdot 10^{16}$ cm^{-3} the value of ρ does not exceed $1 \cdot 10^3$ Ω·cm, while the detector material must be at least 10^{10} Ω·cm. In Fig. 4, there is a rather noticeable increase in charge collection at $N_D(V^+) = 7.5 \cdot 10^{15}$ cm^{-3} for curve *5*. Such an increase occurs at the moment when the Fermi level, in the process of its displacement in the band gap when the concentration of electrically active impurities and defects changes, is far from the energy levels of the traps of nonequilibrium charge carriers. In this case, the capture of charges decreases, and the value of η increases.

During the production of CMT single crystals, background impurities can enter their volume together with the original components, such as interstitial impurities or transition metals, which act as deep donors. This occurs, for example, when CdTe and CdZnTe are produced [20, 21]. Unfortunately, we were unable to find any detailed information on research results of the nature of such impurities in CdMnTe. However, it is possible to investigate the influence of unspecific donor impurities with the different energy levels in the CdMnTe band gap. **Fig. 5** shows the dependences of the charge collection efficiency of the $Cd_{0.9}Mn_{0.1}Te$:V-based detector on the content of deep donors with different energy levels relative to the top of the valence band. The vanadium concentration was taken to be equal to $5.5 \cdot 10^{15}$ cm^{-3}, when resistivity reached the maximal value $\rho \geq 1 \cdot 10^{11}$ Ω·cm, and the content of the studied deep donors varied from $1 \cdot 10^{14}$ to $2 \cdot 10^{16}$ cm^{-3}. For these donor levels the capture cross-section was set within $(1-3) \cdot 10^{-17}$ cm^2.

Fig. 5 shows that the most harmful donor impurities in $Cd_{0.9}Mn_{0.1}Te$ are those with the energy level located within $(E_V + 0.9) - (E_V + 1.2)$ eV in the band gap. Donors with $E_V + 0.4$ eV, which is very close to the energy level of tellurium vacancies in CdTe and CdZnTe [21], reduce charge collection the least. Donor impurities with energy levels of 0.6–0.8 eV relative to the valence band make

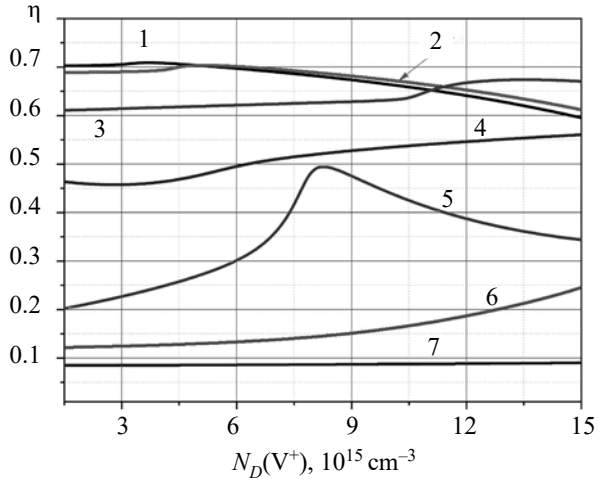

Fig. 4. Dependence of the charge collection efficiency of the detector based on $Cd_{0.9}Mn_{0.1}Te$:V on the content of the vanadium impurity for different concentrations V_{Cd}^{2-}, см$^{-3}$:
1 — $4.1 \cdot 10^{14}$; *2* — $9 \cdot 10^{14}$; *3* — $4 \cdot 10^{15}$; *4* — $9 \cdot 10^{15}$; *5* — $2 \cdot 10^{16}$; *6* — $3 \cdot 10^{16}$; *7* — $5 \cdot 10^{16}$

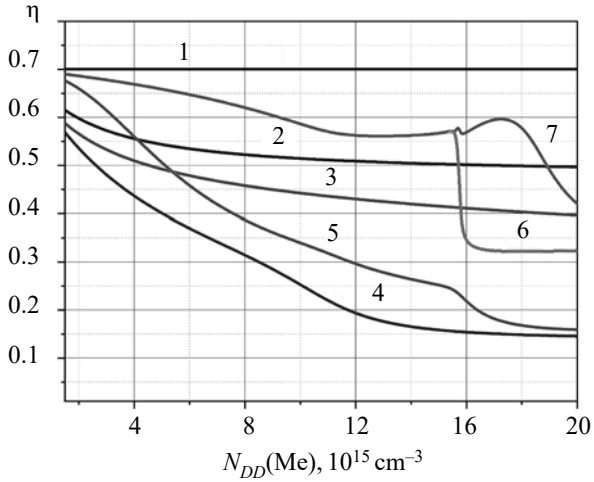

Fig. 5. Dependence of the charge collection efficiency on the concentration of deep donors for their different energy levels relative to the top of valence band, eV:
1 — 0.4; *2* — 0.6; *3* — 0.8; *4* — 1.0; *5* — 1.2; *6* — 1.4; *7* — 1.5

ISSN 2225-5818 (Print)
ISSN 2309-9992 (Online)

a certain contribution to reducing charge collection. T_{12}, T_{13} defects associated with the introduction of manganese and vanadium get to this range. And if at the calculations of η, in addition to the electronic component, we also take into account the hole one, then this value turns out to be even smaller by approximately 0.15 arbitrary units than the one shown in Fig. 5. Thus, the most harmful are impurities that correspond to Ni, Sn, Ge in $Cd_{0.9}Zn_{0.1}Te$ [20]. Vanadium is quite harmful in $Cd_{0.9}Zn_{0.1}Te$ [20], which, by the way, was added to $Cd_{0.9}Mn_{0.1}Te$:V to compensate for cadmium vacancies. It is probably for this reason, the initial value of the charge collection efficiency in the initial state of the studied CMT is noticeably lower ($\eta \approx 0.55$) compared to the mentioned $Cd_{0.9}Zn_{0.1}Te$ ($\eta \approx 0.9$).

We should also take into account the results published in [22], where $Cd_{0.95}Mn_{0.05}Te$:In crystals with the resistivity $\rho = (1.0-2.5)\cdot 10^{10}$ Ω·cm were studied. Mn(99.9998%), Te(6N), CdTe (6N), and In(6N) were used as primary materials. Although the initial raw materials were high-clean, the obtained crystal had a relatively small value $\mu\cdot\tau = 1.7\cdot 10^{-3}$ cm^2/V. The detector based on this material, despite being equipped by Frisch grid, registered the main photopeak of ^{137}Cs at the beam energy $E\gamma$ = 622 keV with a rather coarse (compared to CdZnTe) energy resolution 7.5%. In another experiment [23], on the other hand, the amplitude gamma spectra of a flat $Cd_{0.95}Mn_{0.05}Te_{0.98}Se_{0.02}$:In-based detector irradiated with ^{241}Am had an even worse energy resolution — 11% at the beam energy of 59.5 keV. And after irradiation by ^{57}Co source, the authors of this paper recorded an amplitude spectrum with an even greater blurring of the main photopeak due to a decrease in η.

Thus, based on the results of these studies and our own research, it can be assumed that during the producing of $Cd_{1-x}Mn_xTe$, the introduced manganese not only forms a solid replacement solution, but also some its amount enters the interstitial positions with the formation of point defects and their complexes (associates), which leads to the emergence of deep energy levels acting as traps for nonequilibrium charge carriers. Impurities of vanadium and other elements that have an atomic radius equal to or smaller than that of Cd, Mn, and Te can also play an important role in such process. These electrically active defects, acting as traps, significantly reduce the charge collection efficiency of the detector, and lead to blurring of the main peaks in the amplitude spectra. If this assumption is correct, then it becomes clear why the significant efforts of technologists to purify the raw materials did not give the expected results. In this regard, it is worth focusing further research on elucidating the effect of various donor impurities on the appearance of deep energy levels in the band gap of crystals based on CdMnTe and CdTe and establishing the degree of their influence on the degradation of the detector properties of these materials.

Conclusions

The largest theoretically possible resistivity of $Cd_{0.9}Mn_{0.1}Te$:V at the temperature of 20°C and the deep donor energy $E = E_V + 0.86$ eV can reach $3\cdot 10^{11}$ Ω·cm. Obtaining a detector-quality $Cd_{0.9}Mn_{0.1}Te$ material with $\rho \geq 10^{10}$ Ω·cm requires doping with a donor impurity with an energy level E_{DD} within the range of 0.94 – 0.74 eV relative to the top of the valence band. Change in the content of the donor impurity, which is introduced to compensate for cadmium vacancies, strongly affects ρ, and even its concentration of 10^{16} cm^{-3} can lead to a sharp degradation of the resistivity with a sudden change in the concentrations of electrons and holes. The charge collection efficiency, which is decisive for obtaining amplitude spectra with a high resolution of the main peaks, is noticeably lower in the $Cd_{0.9}Mn_{0.1}Te$-based detector than in the detector based on $Cd_{0.9}Zn_{0.1}Te$. At this stage of technological development, it may be caused not so much by the purity of the constituent components of the produced crystals, but by the nature of the elements that are intentionally introduced into the matrix in order to obtain high detector performance.

Further research should be directed at elucidating the effect of different donor impurities on the occurrence of energy levels inside the band-gap of CdMnTe-based crystals and other CdTe-based materials that fail to get at least as good detector properties as CdZnTe.

REFERENCES

1. Egarievwe S.U., Lukosi E.D., James R.B. et al. Advances in CdMnTe nuclear radiation detectors development. *2018 IEEE Nuclear Science Symposium and Medical Imaging Conference Proceedings (NSS/MIC)*, 2018, pp. 1 – 3. https://doi.org/10.1109/NSSMIC.2018.8824694

2. Pengfei Yu, Yongren Chen, Wei Li et al. Study of detector-grade CdMnTe:In crystals obtained by a multi-step post-growth annealing method. *Crystals*, 2018, vol. 8, iss. 10, p. 387. https://doi.org/10.3390/cryst8100387

3. Lijun Luan, Li Gao, Haohao Lv et al. Analyses of crystal growth, optical, electrical, thermal and mechanical properties of an excellent detector-grade $Cd_{0.9}Mn_{0.1}Te$:V crystal. *Scientific Reports*, 2020, vol. 10, iss. 1, pp. 2749-1 – 2749-10. https://doi.org/10.1038/s41598-020-59612-0

4. Mycielski A., Wardak A., Kochanowska D. et al. CdTe-based crystals with Mg, Se, or Mn as materials for X and gamma ray detectors: Selected physical properties. *Progress in Crystal Growth and Characterization of Materials*, November 2021, vol. 67, iss. 4, p. 100543 https://doi.org/10.1016/j.pcrysgrow.2021.100543

5. Egarievwe S.U., Chan W., Kim K.H. et al. Carbon coating and defects in CdZnTe and CdMnTe nuclear detectors. *IEEE Transaction on Nuclear Science*, 2016, vol. 63, iss. 1, pp. 236 – 245. https://doi.org/10.1109/TNS.2016.2515108

6. Rejhon M., Dědič V., Beran L. et al. Investigation of deep levels in CdZnTeSe crystal and their effect on the internal electric field of CdZnTeSe gamma-ray detector. *IEEE Transaction on Nuclear Science*, 2019, vol. 66, iss. 8, pp. 1952 – 1958. https://doi.org/10.1109/TNS.2019.2925311

7. McCoy J.J., Kakkireni S., Gélinas G. et al. Effects of excess Te on flux inclusion formation in the growth of cadmium zinc telluride when forced melt convection is applied. *Journal of Crystal Growth*, 2020, vol. 535, p. 125542. https://doi.org/10.1016/j.jcrysgro.2020.125542

8. Roy U.N., Camarda G.S., Cui Y. et al. Growth of CdMnTe free of large Te inclusions using the vertical Bridgman technique. *Journal of Crystal Growth*, March 2019, vol. 509, pp. 35 – 39. https://doi.org/10.1016/j.jcrysgro.2018.12.026

9. Vigneshwara P. Raja. Deep-level defects in CdZnTe and CdMnTe detectors identified by photoinduced current transient spectroscopy (PICTS) and thermally simulated current (TSC) techniques. *Technical Report*, October 2020, Indian Institute of Technology Dharwad. https://doi.org/10.13140/RG.2.2.28738.45766

10. Kondrik O.I., Solopikhin D.O. Changes in the electrophysical and detector properties of the promising detector material $Cd_{1-x}Mn_xTe$ depending on the concentration of impurities, defects and manganese content. *Problems of Atomic Science and Technology, series Vacuum, Pure Materials, Superconductors*, Accepted for publication in no. 1, 2024.

11. Kim K. H., Bolotnikov A. E., Camarda G. S. et al. New approaches for making large-volume and uniform CdZnTe and CdMnTe detectors. *IEEE Transaction on Nuclear Science*, 2012, vol. 59, iss. 4, pp. 1510 – 1515. https://doi.org/10.1109/TNS.2012.2202917

12. Kim K., Cho S., Suh J. et al. Gamma-ray response of semi-insulating CdMnTe crystals. *IEEE Transaction on Nuclear Science*, 2009, vol. 56, iss. 3, pp. 858 – 862. http://dx.doi.org/10.1109/TNS.2009.2015662

13. Nykoniuk Ye., Solodin S., Zakharuk Z. et al. Compensated donors in semi-insulating $Cd_{1-x}Mn_xTe$:In crystals. *Journal of Crystal Growth*, October 2018, vol. 500, pp. 117 – 121. https://doi.org/10.1016/j.jcrysgro.2018.08.013

14. Lijun Luan, Yi He, Dan Zheng et al. Defects, electronic properties, and α particle energy spectrum response of the $Cd_{0.9}Mn_{0.1}Te$:V single crystal. *Journal of Materials Science: Materials in Electronics*, 2020, vol. 31, pp. 1179 – 4487. https://doi.org/10.1007/s10854-020-02996-6

15. Novikov G.F., Radychev N.A. Experimental determination of the dependence of the free electron-hole recombination rate constant on the band gap in semiconductors of the $A^{II}B^{VI}$ and $A^{I}B^{VII}$ types. *Russian Chemical Bulletin*, 2007, vol. 56, pp. 890 – 894. https://doi.org/10.1007/s11172-007-0134-9

16. Shockley W., Read W.T. Statistics of the recombinations of holes and electrons. *Physical Reviev*, 1952, vol. 87, iss. 5, pp. 835 – 842. https://doi.org/10.1103/PhysRev.87.835

17. Kondrik A. I., Kovtun G. P. Influence of impurities and structural defects on electrophysical and detector properties of CdTe and CdZnT. *Technology and design in electronic equipment*, 2019, no. 5 – 6, pp. 43 – 50. https://dx.doi.org/10.15222/TKEA2019.5-6.43 (Rus)

18. Knoll G. F. Radiation detection and measurement. J*ohn Wiley & Sons, Inc*., 2010, 864 p.

19. Petrus R.Yu., Ilchuk H.A., Sklyarchuk V.M.et al. Transformation of band energy structure of solid solutions CdMnTe. *Journal of Nano- and Electronic Physics*, 2018, vol. 10, iss. 6, p. 06042. https://doi.org/10.21272/jnep.10(6).06042

20. Kondrik A. I., Kovtun G. P. Influence of impurities and structural defects on the properties of CdTe- and CdZnTe-based detectors. *Technology and design in electronic equipment*, 2022, iss. 1 – 3, pp. 31 – 38. http://dx.doi.org/10.15222/TKEA2022.1-3.31 (Ukr)

21. Hofmann D. M., Stadler W., Christmann P., Meyer B. K. Defects in CdTe and $Cd_{1-x}Zn_xTe$. *Nuclear Instruments and Methods in Physics Research Section A*, 1996, vol. 380, iss. 1 – 2, pp. 117 – 120. https://dx.doi.org/10.1016/S0168-9002(96)00287-2

22. Roy U.N., Okobiah O.K., Camarda G.S., et al. Growth and characterization of detector-grade CdMnTe by the vertical Bridgman technique. *AIP Advances*, 2018, vol. 8, p. 105012. https://doi.org/10.1063/1.5040362

23. Byun J., Seo J., Seo J., Park B. Growth and characterization of detector-grade CdMnTeSe. *Nuclear Engineering and Technology*, November 2022, vol. 54, iss. 11, pp. 4215 – 4219 https://doi.org/10.1016/j.net.2022.06.007

Received 10.09 2023

DOI: 10.15222/TKEA2023.3-4.52
УДК 621.315.592.3

О. І. КОНДРИК, Д. О. СОЛОПІХІН

Україна, ННЦ «Харківський фізико-технічний інститут»
E-mail: kondrik@kipt.kharkov.ua

ПЛИВ ВМІСТУ ДОМІШОК ТА СТРУКТУРНИХ ДЕФЕКТІВ НА ВЛАСТИВОСТІ ДЕТЕКТОРА НА ОСНОВІ $Cd_{0.9}Mn_{0.1}Te$:V

Досліджено перспективний матеріал $Cd_{0.}9Mn_{0.1}Te$:V, призначений для працюючих за кімнатної температури детекторів рентгенівського та гамма-випромінювання. Отримано результати кількісних досліджень впливу вмісту домішок та структурних дефектів на електрофізичні та детекторні властивості $Cd_{0.9}Mn_{0.1}Te$:V. Проведено аналіз обчислених величин питомого опору ρ та концентрацій вільних носіїв заряду, часу життя нерівноважних носіїв заряду τ, ефективності збирання зарядів η за різного складу домішок та дефектів у цьому матеріалі за температури 20°C. Встановлено оптимальні діапазони зміни енергії E_D та концентрації глибокого донора N_D, які забезпечують високоомний стан й прийнятні величини τ та η. Досліджено компенсацію вакансій кадмію домішкою ванадію. Зроблено припущення щодо причини відносно малої величини η та низької роздільності основних фотопіків в амплітудних спектрах детекторів на основі CdMnTe. Сформульовано напрямок подальших досліджень з метою з'ясування конкретних чинників деградації детекторних властивостей матеріалу під впливом внесених та фонових домішок.

Ключові слова: CdMnTe, властивості детектора, моделювання, дефекти структури, глибокі рівні.

Опис статті для цитування:

Кондрик О. І., Солопіхін Д. О. Вплив вмісту домішок та структурних дефектів на властивості детектора на основі $Cd_{0.9}Mn_{0.1}Te$:V. Технологія та конструювання в електронній апаратурі, 2023, № 3 – 4, с. 52–58. http://dx.doi.org/10.15222/TKEA2023.3-4.52

Cite the article as:

Kondrik O. I., Solopikhin D. A. Influence of the content of impurities and structural defects on the properties of the $Cd_{0.9}Mn_{0.1}Te$:V-based detector. Technology and design in electronic equipment, 2023, no. 3 – 4, pp. 52–58. http://dx.doi.org/10.15222/TKEA2023.3-4.52

ISSN 2225-5818 (Print)
ISSN 2309-9992 (Online)